Journal of Sound and Vibration (2002) **254**(3), 503–521
doi:10.1006/jsvi.2001.4098, available online at http://www.idealibrary.com on IDEAL®

MODELLING OF VIBRATING SYSTEMS USING TIME-DOMAIN FINITE ELEMENT METHOD

J. SUK

Department of Aerospace Engineering, Chungnam National University, Daejeon 305-764 *Korea.*
E-mail: jsuk@cnu.ac.kr

AND

Y. KIM†

Department of Aerospace Engineering, Seoul National University, Seoul 151-742 *Korea.*
E-mail: ydkim@snu.ac.kr

(*Received* 4 *June* 2001, *and in final form* 15 *October* 2001)

In this paper, several dynamic systems are modelled using the time-domain finite element method. Galerkin's weak principle is used to model the general second order mechanical system, and is applied to the dynamics of the simple pendulum. Problems that arise during the approximation of the final momentum are also investigated. Furthermore, additional dynamic analysis methods are suggested for hybrid co-ordinate systems that have both slew and flexible modes. The proposed methods are based on both extended Hamilton's principle and Galerkin's weak principle. The matrix wave equation is propagated in a space domain, satisfying the geometric/natural boundary conditions. As a result, the flexible motion can be obtained, and this was compatible with the applied control input. A numerical example is used to demonstrate the effectiveness of the proposed modelling methods for the hybrid co-ordinate systems.

1. INTRODUCTION

Over the past few decades, much research work has been undertaken on numerical implementation tools for dynamic analysis after Bailey's reinvestigation of Hamilton's Principle, which is also known as Hamilton's law [1]. It is necessary to clearly describe the boundary conditions in order to apply the temporal finite element method to dynamic systems. This is because dynamic system analysis always involves the initial value problems as opposed to the various applications of the conventional space-domain finite element method. Generally, in terms of conditions, the values of displacement and momentum are specified at the initial stage. However, we cannot define the final co-ordinates except in the case of special dynamic problems. It should be noted that this final momentum should be neither neglected nor approximated by temporal finite elements. Numerous research programs have been undertaken to deal with this constraint, the references cited represent examples only [2–6]. A general approach to the direct formulation of this kind of problem involves a progressive time marching technique, that performs the same role as numerical integration. Hodges and Bless [7], and Lee and Kim [8] expanded Hamilton's weak principle and applied it to the dynamics and optimization of mechanical systems described

†The Institute of Advanced Aerospace Technology

0022-460X/02/$35.00

in the state-space formulation. Variation of the performance index and the temporal finite-element discretization of the state/costate equation produce finite-dimensional non-linear algebraic equations, and result in the optimal trajectory of the dynamic systems. A systematic optimization can be directly applied to the real-time guidance of the launch vehicle. Warner and Hodges [9] showed that either lower or higher order shape functions can be used for time discretization; however, there exist limitations for real-time implementation in higher order polynomials, whilst guaranteeing the improvement accuracy. Kim and Cho [10] formulated the initial value problems using a weighted penalty method that is compatible with the parallel computing system environment. Öz and Adigüzel [11] suggested an algebraic equation of motion using Hamilton's law in combination with assumed time modes. The modelling method is well suited to a direct optimal control strategy of general dynamic systems [12]. A new analytic approach to Hamilton's law is suggested for the dynamic analysis of linear systems using the fundamental time modes and linear system theories [13]. The analyses of the deterministic dynamics are extended to accommodate the dynamic systems subject to random excitation in a stochastic perspective [14].

Flexible space structures or articulated robot arms are subject to slew motion centered at their axle. The system exhibits two modes: (1) a slew mode represented by the rotational motion of the whole system, and (2) a flexible mode resulting from structural flexibility coupled with the slew motion. An accurate and effective method to describe this kind of hybrid co-ordinate system involves discretizing the structure by the conventional (space-domain) finite element method [15, 16]. Slew mode is coupled with the flexible mode resulting in combined mass, stiffness and input matrices from the point of view of the conventional finite element method. On the other hand, the temporal finite element method based on Hamilton's weak principle can be readily applied to dynamic systems that have only time-dependent variables. However, it is complicated to analyze the dynamics of distributed parameter systems, which are dependent on both time and space variables. To overcome these problems, space domain was discretized using a conventional finite element method. The resulting matrix differential equation is similar to that of a second order mechanical system. Once the system is time dependent, Hamilton's weak principle can be applied. Another direct method is to apply the space–time finite element method (STFEM) that discretizes both the spatial and time domains [17–19]. These general approaches generally produce good results, which are accepted for solving the dynamics of distributed parameter systems. However, they are subject to a routine job and generally require a relatively significant amount of computation, which depends on the number of finite elements used in the space and time domains.

Flowtow and Schäer [20] proposed the wave domain method to analyze the dynamic behavior of structures subject to external input. This method freezes the time domain and analyzes the structural system in the space domain. Subsequently, the wave absorbing control strategy can be used for the frequency domain approach, by using either the Fourier transformation [20, 21] or the Laplace transformation [22, 23] of the governing equation. Motivated by wave propagation and absorbing control, this paper presents a numerical realization of the spatial propagation of the hybrid co-ordinate systems using the time-domain finite element method. To achieve this, a closed-form matrix construction, not the progressive time marching method, in the time domain is required. In the first part of this paper, a closed-form algebraic matrix equation of motion is formulated using Galerkin's approach with an appropriate matrix construction. Note that the proposed formulation is still in the category of Galerkin's general approach and has a role equivalent to Hamilton's formulation. It is shown that the appropriate matrix construction results in algebraic equations, and consequently, the overall solution can be obtained by a simple inversion.

Another example demonstrates that the approximation of final momentum gives rise to accumulated errors in terms of the overall system response.

Although the matrix algebraic equation has a closed form, it is unsuitable for direct application to the spatial propagation of a flexible structure, and therefore, another time-domain analysis method is proposed in the latter part of this paper for hybrid co-ordinate systems that have additional spatial dimension, subject to the rest-to-rest maneuver. The dynamic analysis of the slewing hybrid co-ordinate systems is performed for the case that the initial and final momenta are specified so that the constructed state-space equation preserves the same eigensystem characteristics as those in the frequency-domain analysis of the previous works [20]. Both the extended Hamilton's principle and Galerkin's weak principle are used to formulate the system. A Spatial Propagation equation based on these formulations enables a flexible mode solution, which extends the well-identified method for cantilevered structures [24]. As a result of time discretization, the flexible mode equation is reduced to a fourth order matrix differential equation, which is a function of the slew motion, whereas slew motion is converted into an algebraic matrix equation that incorporates the effects of the flexible mode and control input. The hybrid co-ordinate system used in this study is composed of four flexible appendages attached to a central hub, which rotates around the vertical axis.

This paper is organized as follows. First, the dynamic modelling of a general non-conservative mechanical system is presented using the time-domain finite element method. The modelling methods are validated by a double integrator problem, and the effect of the approximation of the final momentum is also investigated. Dynamic analyses of the hybrid co-ordinate systems are presented using both the extended Hamilton's principle and Galerkin's weak principle. Finally, a numerical example is provided to compare the effectiveness of the proposed methods.

2. TIME-DOMAIN FEM APPLIED TO THE DYNAMIC SYSTEMS

In this section, the dynamic system is modelled using Galerkin's weak principle and it is shown that the modelling method is equivalent to that obtained using Hamilton's weak principle. Several numerical examples are used to investigate the modelling method, namely: dynamics as a time sequence, open- and closed-loop system dynamics. The effect of the final momentum approximation on the numerical result is also investigated. Galerkin's weak principle starts from a dynamic equation of motion while Hamilton's weak principle starts from the energy relationships of a dynamic system. It is also noted that the variation in Hamilton's weak principle has the same role as the weighting function in Galerkin's weak principle.

2.1. FORMULATION

The dynamic equation of motion for the second order non-conservative mechanical system can be expressed as follows:

$$m\ddot{v}(t) + c\dot{v}(t) + kv(t) = u(t), \tag{1}$$

where m, c, k, $v(t)$ and $u(t)$ denote the mass, damping, stiffness coefficients, displacement, and external excitation input, respectively, and $(\cdot)$ denotes differentiation with respect to time. The initial conditions are $v_0 = k^{-1}u_0$, $p_0 = m\dot{v}_0$, where p_0 denotes the initial momentum of the system. Mathematical manipulations of equation (1) yield the weak finite element formulation as follows:

$$-\int_{t_0}^{t_f} m\dot{v}(t)\dot{\eta}(t)\,\mathrm{d}t + \int_{t_0}^{t_f} c\dot{v}(t)\eta(t)\,\mathrm{d}t + \int_{t_0}^{t_f} kv(t)\eta(t)\,\mathrm{d}t = \int_{t_0}^{t_f} u(t)\eta(t)\,\mathrm{d}t - p(t)\eta(t)\Big|_{t_0}^{t_f}, \tag{2}$$

where $\eta(t)$ is an unknown weight function and $p(t) = m\dot{v}(t)$ is the momentum of the system. The variables $v(t)$ and $\eta(t)$ can be discretized as follows using the time-based shape functions.

$$v(t) = \sum_i \phi_i(t) v_i, \qquad \eta(t) = \sum_j \phi_j(t) \eta_j, \tag{3}$$

where the weight function is chosen in the basis functions that are identical to the trial function [25]. In equation (2), the conditions for the state variables and the weighting function are attenuated so that their first derivatives are continuous. This enables us to use the first or higher order polynomials as shape functions; for example, the Lagrange polynomials are suitable as shape functions because their first derivatives are continuous. The sum of shape functions at any instance is unity and the sum of their derivatives becomes zero, which is often used to confirm the adopted shape functions. Using equations (2) and (3) the finite element formulation of the dynamic system can be obtained as follows:

$$-M\mathbf{v} + C\mathbf{v} + K\mathbf{v} = F, \tag{4}$$

where

$$\mathbf{v} = [v_0,\ v_1\ \cdots\ v_N\ p_f]^{\mathrm{T}} \quad M = \begin{bmatrix} 0_{1,N+1} & 0 \\ M^e & 0_{N+1,1} \end{bmatrix} \quad C = \begin{bmatrix} 0_{1,N+1} & 0 \\ C^e & 0_{N+1,1} \end{bmatrix},$$

$$K = \begin{bmatrix} \begin{bmatrix} \int_{t_0}^{t_f} k\,\mathrm{d}t\ 0_{1,N} \end{bmatrix} & 0 \\ K^e & \begin{bmatrix} 0_{N,1} \\ 1 \end{bmatrix} \end{bmatrix}, \quad F = \begin{bmatrix} \int_{t_0}^{t_f} u_0\,\mathrm{d}t + p_0 \\ F^e \end{bmatrix},$$

$$M_{ij}^e = \int_{\Delta t} m\dot{\phi}_i(t)\dot{\phi}_j(t)\mathrm{d}t,\ C_{ij}^e = \int_{\Delta t} c\dot{\phi}_i(t)\phi_j(t)\mathrm{d}t,$$

$$K_{ij}^e = \int_{\Delta t} k\phi_i(t)\phi_j(t)\,\mathrm{d}t,\ F_i^e = \int_{\Delta t} u(t)\phi_i(t)\,\mathrm{d}t - \int_{\Delta t} u_0\phi_i(t)\,\mathrm{d}t,$$

where p_0 is added to the first row of F in order to reflect the initial momentum, and the final momentum p_f is subtracted from the last row. Since p_f is unknown, it is augmented in the state vector, and therefore, the overall number of states is $(N + 2)$ where N is the number of finite elements in time multiplied by the order of the adopted shape functions.

The displacement can be obtained from equation (4) as

$$\mathbf{v} = (-M + C + K)^{-1} F. \tag{5}$$

Note that the term inside the parentheses is usually invertible. The system order is $(N + 2)$, while both matrices M and C have 1-degeneracy, which is caused by the augmentation. However, the matrix K has full rank making the overall matrix also have full rank. The condition of the matrix K becomes worse as the number of finite elements in time increases. However, the condition number of $(-M + C + K)$ is moderate and almost independent of the number of finite elements. Therefore, the combined matrices are appropriately conditioned and the overall matrix is invertible.

2.2. HAMILTON'S WEAK PRINCIPLE

Another formulation using Hamilton's weak principle can be obtained from the variation of the Lagrangian on the basis of the global energy relationship of the conservative/non-conservative mechanical systems [6]. The following variational equations were derived

using the D'Alembert and virtual work principle as a function of generalized co-ordinate, velocity, and time:

$$-\int_{t_0}^{t_f}\{\delta L(q,\dot{q},t)+\delta q^{\mathrm{T}}Q\}\mathrm{d}t=\delta q^{\mathrm{T}}p|_{t_0}^{t_f}, \tag{6}$$

where q, $p=\partial L/\partial\dot{q}$, L, and Q denote a generalized co-ordinate, a generalized momentum, the Lagrangian of the system, and non-conservative force, respectively. Generalized co-ordinates and velocity are discretized for each finite time interval by

$$q(t)=\sum_i \phi_i(t)q_i, \qquad \dot{q}(t)=\sum_i \dot{\phi}_i(t)q_i, \tag{7}$$

A total of $n+1$ algebraic equations are derived for the nth order shape function from equations (6) and (7), from which the subsequent displacement and momentum for each time step are obtained. The displacement and velocity of the next time step can be obtained recursively using the final displacement and momentum of the previous time finite element.

2.3. NUMERICAL EXAMPLES

2.3.1. *Dynamic analysis of the open-loop and closed-loop systems*

In order to validate the time domain finite element method using Galerkin's weak principle, the undamped simple pendulum shown in Figure 1 was investigated. A linearized equation of motion around the equilibrium state can be described as follows:

$$\ddot{v}(t)+\frac{g}{l}v(t)=u(t), \tag{8}$$

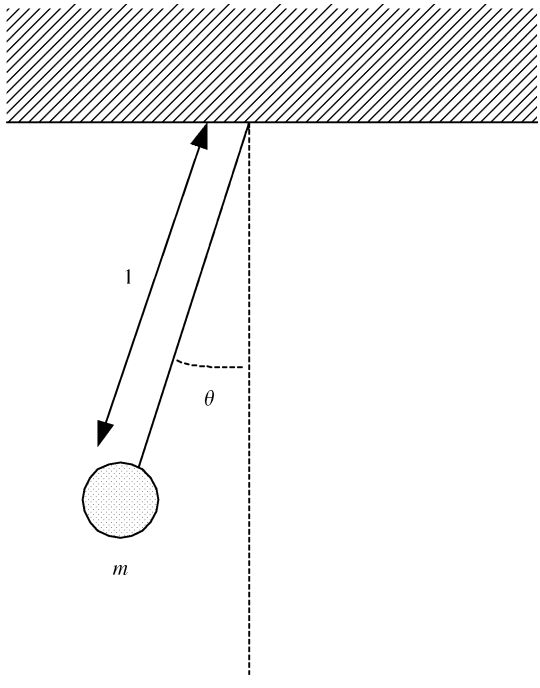

Figure 1. A simple pendulum.

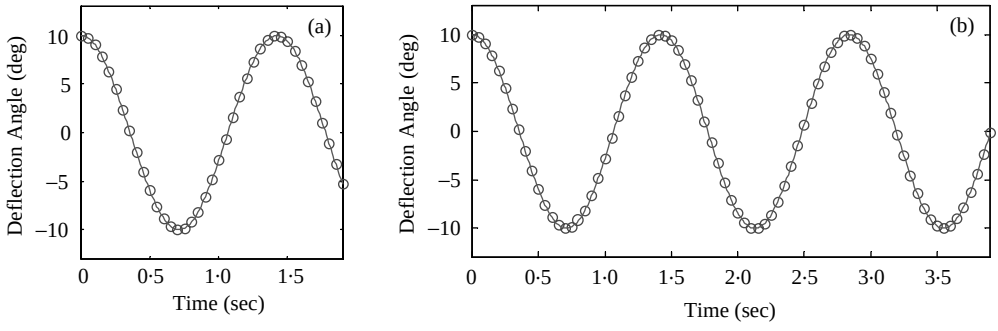

Figure 2. Free response of a simple pendulum: (a) simulation time of 2 s; (b) simulation time of 4 s.

where g is the gravitational constant and the length of pendulum is $l = 0{\cdot}5\,\mathrm{m}$. In this example, $v_0 = 10^\circ$ and $p_0 = 0$ are chosen as the initial conditions. Figure 2 shows the open-loop response of the angular displacement when there is no external input with a time interval of 0·1 s. Since the damping factor is not considered in this example, the displacement history shows a periodic motion with the period of about 1·4 s. Figure 2(a) and 2(b) shows the results for different final times, and therefore it is confirmed that the modelling method is not dependent on a special time or state of the system. This method is unconditionally stable and the existence of an inverse matrix produces accurate results even for a large time interval. The meaning of "unconditionally stable" in this paper did not originate from a direct derivation from the general time integration scheme. Spectral radius of the method is not directly obtained from the finite difference relationship of the explicit or implicit integration. In time-domain finite element method, the effect of stability exists implicitly in the matrices M and K. Therefore, the time-marching relationship is only implied in the process of generation of the element matrices. Note that the momentum can be obtained at each time step in Hamilton's weak principle, while it must be obtained via post-processing work after the displacement history is determined in Galerkin's weak principle.

Closed-loop system dynamics was also investigated for the mechanical system with the following state feedback:

$$u(t) = -k_1 v(t) - k_2 \dot{v}(t). \tag{9}$$

Substituting equation (9) into equation (8) yields

$$\ddot{v}(t) + k_2 \dot{v}(t) + \left[\frac{g}{l} + k_1\right] v(t) = 0. \tag{10}$$

Therefore, the response of the closed-loop system can be obtained using a similar procedure. Figure 3 shows the time history of the closed-loop system for the various feedback gains with the same initial conditions. It is evident that the velocity feedback has a dominant role in the regulation while the displacement feedback increases the bandwidth.

2.3.2. *Approximation of the final momentum*

Special attention should be given to the approximation of final momentum, because even a normal approximation of the final momentum can lead to the wrong results. In this section, it is shown that the momentum approximation may produce inconsistent results.

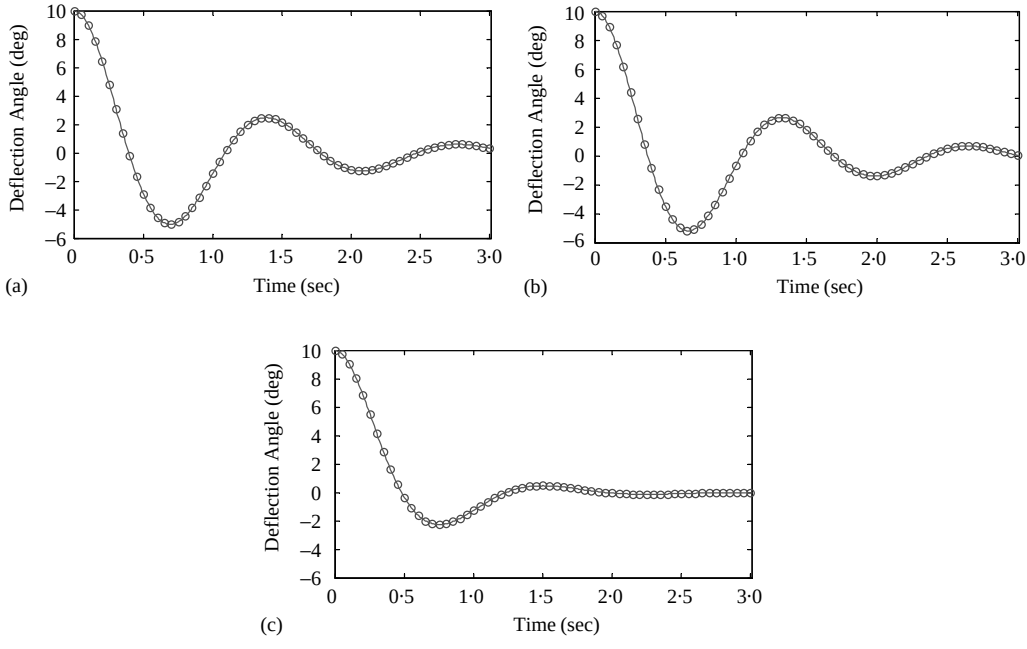

Figure 3. Closed-loop response of a simple pendulum; (a) $k_1 = 2$, $k_2 = 2$; (b) $k_1 = 4$, $k_2 = 2$; (c) $k_1 = 2$, $k_2 = 4$.

Let us assume that the final momentum can be approximated in the time domain as follows:

$$p_f = m\sum_i \dot{\phi}_i(t_f)v_i. \tag{11}$$

Substituting equation (11) into equation (2) makes the final momentum move to the left side of equation (2) and locate the last row of the matrix M, thus reducing the number of states. For example, taking a second order Lagrange polynomial as a shape function and using only one temporal finite element, the final momentum can be expressed for a unit mass as follows:

$$p_f = \frac{1}{\Delta t}\begin{bmatrix}1 & -4 & 3\end{bmatrix}\begin{bmatrix}v_0\\ v_1\\ v_2\end{bmatrix} \tag{12}$$

or

$$p_f = \frac{1}{\Delta t}\begin{bmatrix}-1 & \frac{9}{2} & -9 & \frac{11}{2}\end{bmatrix}\begin{bmatrix}v_0\\ v_1\\ v_2\\ v_3\end{bmatrix} \tag{13}$$

when a third order Lagrange polynomial is used.

As shown in Figure 4, results using equations (12) and (4) mislead the overall trajectory. Note from Fig. 4(b) that the result is not dependent on the order of the shape function. The approximated formulation is subjected to the inversion process of equation (5) and the small error in the first finite element is accumulated as it proceeds, leading to the unexpected results.

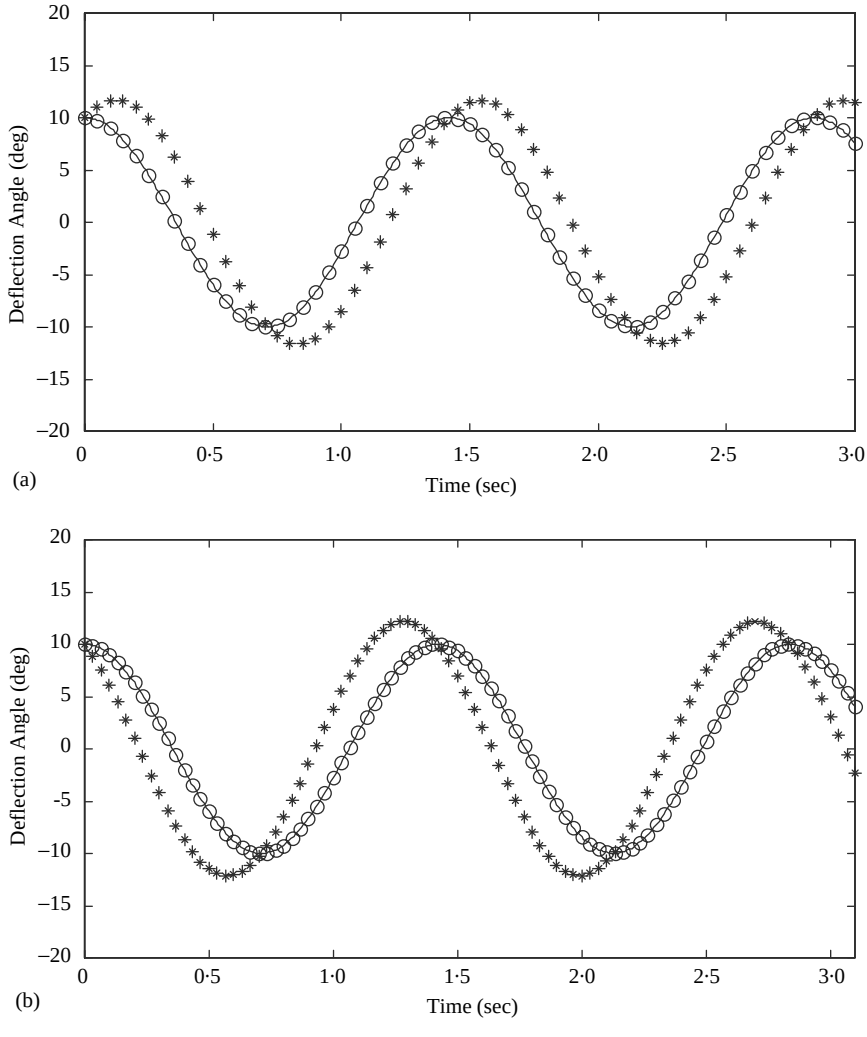

Figure 4. Free response of a simple pendulum: *: final momentum not approximated; **: final momentum approximated; (a) Quadratic polynomial; (b) cubic polynomial: ○ time domain FEM*; * time domain FEM**; —— numerical simulation.

3. DYNAMIC ANALYSIS OF THE HYBRID CO-ORDINATE SYSTEMS

3.1. EXTENDED HAMILTON'S PRINCIPLE

In the previous section, the time domain finite element method incorporating Galerkin's weak principle was introduced to analyze a general second order mechanical system, and compared with Hamilton's weak principle, and was demonstrated for cases involving simple mechanical systems. In the following sections, dynamic modelling of hybrid co-ordinate systems is investigated in the time domain. The Hub-appendage system shown in Figure 5 is considered, and flexible appendages are subjected to elastic deformation in the hybrid co-ordinate systems. A torque generator is mounted on the central hub and a distributed force actuator is attached to the appendage to control the flexible motion. It is

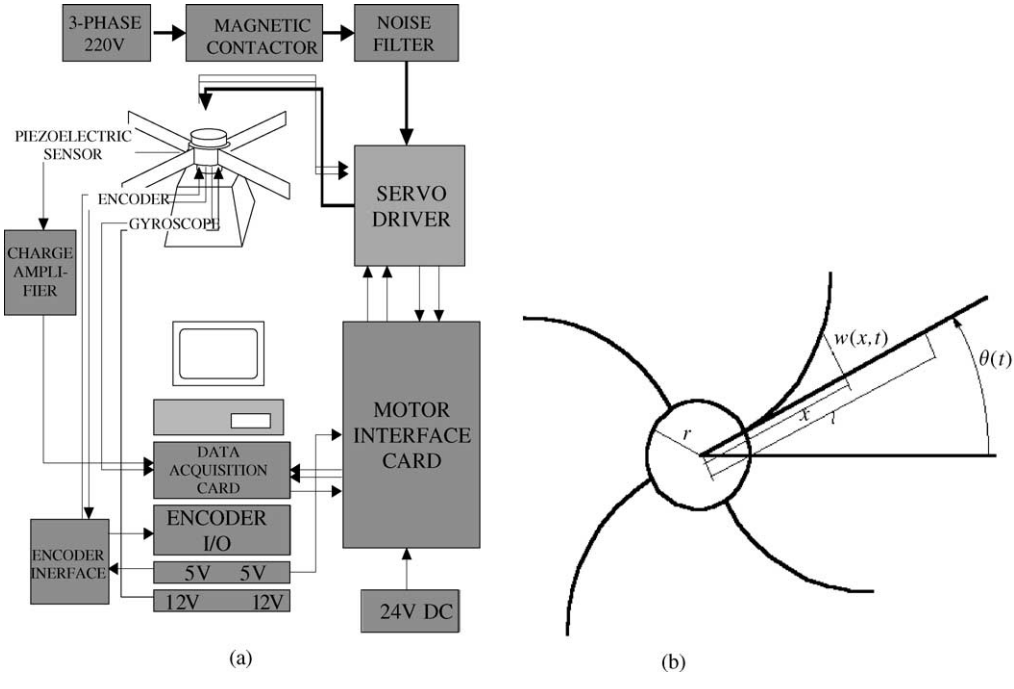

Figure 5. Hybrid co-ordinate system: (a) integrated structure-control signal flow diagram; (b) co-ordinate system (top view).

assumed that the final momentum becomes negligible, which is the general case for a controlled rest-to-rest maneuver.

3.1.1. *Time discretization*

In this section, general co-ordinates are discretized based on the extended Hamilton's principle. The slew mode can be treated like the flexible co-ordinates, and therefore, it can be entered inside the integration. The total kinetic and potential energy of the hybrid co-ordinate system can be expressed as follows [26]:

$$T = \frac{1}{2}J_h\dot{\theta}^2 + 4\cdot\frac{1}{2}\int_r^l \rho(x)[\dot{w}(x,t) + x\dot{\theta}(t)]^2\,\mathrm{d}x, \tag{14}$$

$$P = 4\cdot\frac{1}{2}\int_r^l EI\left\{\frac{\partial^2 w(x,t)}{\partial x^2}\right\}^2\,\mathrm{d}x, \tag{15}$$

where x is a spatial variable measured from the center of the hub along the undeformed appendage axis, $\theta(t)$, $w(x, t)$, J_h, r, and l are the slew angle, the transverse deflection of the appendage measured from the x-axis, the hub moment of inertia, the radius of hub, and the distance between the center of hub and the tip of appendage respectively. The virtual work imposed by the hub-mounted exciter and the distributed force actuator is given by

$$\delta W = u_r(t)\delta\theta(t) + 4\int_r^l f(x,t)\delta w(x,t)\,\mathrm{d}x. \tag{16}$$

To apply the extended Hamilton's principle to the hub-appendage model, let us take the variation on the integrand and integrate the resulting equation over finite time, as follows:

$$\int_{t_0}^{t_f}\Bigg\{J_h\dot{\theta}(t)\delta\dot{\theta}(t)+u_r(t)\delta\theta(t)+4\int_r^l\rho[\dot{w}(x,t)+x\dot{\theta}(t)]\,[\delta\dot{w}(x,t)+x\delta\dot{\theta}(t)]\,\mathrm{d}x \\ -4\int_r^l EIw''(x,t)\delta w''(x,t)\,\mathrm{d}x+4\int_r^l f(x,t)\delta w(x,t)\,\mathrm{d}x\Bigg\}\,\mathrm{d}t=0. \tag{17}$$

In the above equation, all terms are included in the time integration; however, the slew mode remains outside the spatial integration. All the modes should be included in the spatial integration in order to deduce the equation from equation (17). Therefore, the slew mode and the hub torque-related terms are included in the spatial integration with some manipulation as follows:

$$\int_{t_0}^{t_f}\int_r^l\Bigg\{\frac{3x^2}{l^3-r^3}J_h\dot{\theta}(t)\delta\dot{\theta}(t)+\frac{3x^2}{l^3-r^3}u_r(t)\delta\theta(t)+4\rho[\dot{w}(x,t)+x\dot{\theta}(t)]\,[\delta\dot{w}(x,t)+x\delta\dot{\theta}(t)] \\ -4EIw''(x,t)\delta w''(x,t)+4f(x,t)\delta w(x,t)\Bigg\}\,\mathrm{d}x\,\mathrm{d}t=0. \tag{18}$$

Now, a new variable is defined such that the slew mode can be propagated into the spatial domain:

$$\xi(x,t)=\theta(t)x. \tag{19}$$

Using equation (19), equation (18) can be rewritten as

$$\int_r^l\int_{t_0}^{t_f}\Bigg\{\left[4\rho+\frac{3J_h}{l^3-r^3}\right]\dot{\xi}(x,t)\delta\dot{\xi}(x,t)+4\rho\dot{\xi}(x,t)\delta\dot{w}(x,t)+4\rho\dot{w}(x,t)\delta\dot{\xi}(x,t)+4\rho\dot{w}(x,t)\delta\dot{w}(x,t) \\ -4EIw''(x,t)\delta w''(x,t)+\frac{3x}{l^3-r^3}u_r(t)\delta\xi(x,t)+4f(x,t)\delta w(x,t)\Bigg\}\,\mathrm{d}t\,\mathrm{d}x=0. \tag{20}$$

The slew and flexible modes are discretized as a general consequence of the finite element discretization in time as follows:

$$\xi(x,t)=\sum_i\psi_i(t)\xi_i(x),\qquad w(x,t)=\sum_j\phi_j(t)w_j(x). \tag{21}$$

Note that the basis functions, $\psi_i(t)$ and $\phi_j(t)$, for each co-ordinate may have different orders. However, this would result in either an under-determined or an over-determined algebraic equation so that another assumption and/or approximation should be provided. Therefore, the same order of shape functions was used, i.e., $\psi_i(t)=\phi_i(t)$.

In this study, it is assumed that the distributed force on the appendage is a function of independent time and space variables as follows:

$$f(x,t)=u_d(t)\,f_d(x). \tag{22}$$

An ideally distributed force actuator might be considered to have an arbitrary control sequence on any position of the appendage. However, this would be unrealistic because an infinite-dimensional actuator is required. On the other hand, the above assumption of equation (22) is valid in the sense that we can tailor the force distribution appropriately along the appendage using the area of the attached actuator. Once the force distribution is determined, the actuator can be activated by either open-loop control or state feedback

control. Under this assumption, the complete matrix of ordinary differential equations is obtained as follows:

$$-M_a X + K_a X^{(iv)} = F_a \begin{pmatrix} f_r(x) \\ f_d(x) \end{pmatrix}, \tag{23}$$

where,

$$M_a = \begin{bmatrix} M_{\theta\theta} & 4M_{\theta w}^{\mathrm{T}} \\ 4M_{\theta w} & 4M_{ww} \end{bmatrix}, \quad K_a = \begin{bmatrix} 0 & 0^{\mathrm{T}} \\ 0 & 4K_{ww} \end{bmatrix}, \quad F_a = \begin{bmatrix} F_r & 0 \\ 0 & 4F_d \end{bmatrix}, \quad X = \begin{bmatrix} \xi(x) \\ w(x) \end{bmatrix}.$$

Note that the matrices M_a and K_a preserve symmetry. When the element matrices are symmetric, the computational load can be substantially reduced. In the case of mechanical second order systems, the algebraic equation can be solved with almost half the original variables. Moreover, in the case of this spatial matrix differential equation, the real co-ordinates can be transformed into the time-mode modal co-ordinates by solving the generalized eigenvalue problems. The characteristics of the time-mode modal co-ordinate have a significant meaning in the analysis. That is, the time mode model reduction can be implemented so that only a small number of time modes are used to describe the dynamic motion of the system. The submatrices can be computed by integrating the shape functions and their first time derivatives in combination with the configuration parameters of the system as follows:

$$\begin{aligned}
[M_{\theta\theta}]_{ij} &= \int_{\Delta t} \left\{ 4\rho + \frac{3J_h}{l^3 - r^3} \right\} \dot{\psi}_i(t)\dot{\psi}_j(t)\,\mathrm{d}t, \\
[M_{\theta w}]_{ij} &= \int_{\Delta t} \rho \dot{\psi}_i(t)\dot{\phi}_j(t)\,\mathrm{d}t, \\
[M_{ww}]_{ij} &= \int_{\Delta t} \rho \dot{\phi}_i(t)\dot{\phi}_j(t)\,\mathrm{d}t, \\
[K_{ww}]_{ij} &= \int_{\Delta t} EI\phi_i(t)\phi_j(t)\,\mathrm{d}t, \\
[F_r]_i &= \frac{3}{l^3 - r^3} \int_{\Delta t} u_r(t)\psi_i(t)\,\mathrm{d}t, \\
[F_d]_i &= \int_{\Delta t} u_d(t)\phi_i(t)\,\mathrm{d}t,
\end{aligned} \tag{24}$$

and $f_r(x)$ in equation (23) is the spatial distribution of the external torque actuated on the central hub, $\xi_i(x) = \theta_i x$ varies linearly in the spatial domain, where $\boldsymbol{\theta}_i$ denotes the slew angle at the ith time step, and finally, $w(x)$ denotes the time history of elastic deformation of the appendage.

Note that the notations in equation (24) have similar forms to the conventional (space-domain) finite element method. However, the definition is actually totally different. That is, the matrices $M_{\theta\theta}$, $M_{\theta w}$, M_{ww} and K_{ww} are mass-weighted and stiffness-weighted influence matrices in the time domain. A combination of the matrices shown in equation (5) represents how exactly the dynamic behavior of the system is described. They are related with only the time domain, not the spatial domain, although it has only a small effect on the spatial domain by way of the time-based generalized eigenvalues and eigenvectors. Spatial domain analysis can be performed by utilizing the fourth order matrix differential equation after transforming it into the state-space form, as shown in the next section.

3.1.2. *Spatial propagation*

In this section, the spatial propagation of the matrix wave equation is investigated for the hybrid co-ordinate systems. Note that the slew mode is not influenced by the spatial propagation. If the flexible appendage is assumed to be a rigid body and only the slew motion is considered, then the resulting matrix equation would be an algebraic equation so that the slew response can be obtained simply by an inversion, as described for the case in section 2. However, when the flexibility is considered, the spatial propagation in the flexible mode should be built. Special attention should be given in order to obtain the slew motion from the coupled slew-flexible interaction. In this study, the same finite element basis functions are used for both slew and flexible modes, then the submatrices consisting of M_a and K_a become square matrices with the same dimension. In particular, $M_{\theta w}$ is a square matrix equivalent to M_{ww} while $M_{\theta\theta}$ is a scalar multiple of M_{ww}. We further assumed that the hub control torque is the only external control input applied to the system. Then, equation (23) can be divided into two matrix equations and the spatial propagation in the flexible mode is represented in combination with matrices M_{ww}, K_{ww} and F_r as follows:

$$-\frac{J}{\rho}M_{ww}\mathbf{w}(x)+\left[4+\frac{J}{\rho}\right]K_{ww}\mathbf{w}^{(iv)}(x)=-F_r\,x, \tag{25}$$

where $J = 3J_h/(l^3 - r^3)$.

Equation (25) can be written in the first order state-space form as

$$y'(x) = A\,y(x) + Bx, \tag{26}$$

where

$$y=\begin{bmatrix}\mathbf{w}(x)\\ \mathbf{w}'(x)\\ M_B(x)\\ V(x)\end{bmatrix},\quad A=\begin{bmatrix}0 & \mathbf{I} & 0 & 0\\ 0 & 0 & \dfrac{1}{EI}\mathbf{I} & 0\\ 0 & 0 & 0 & \mathbf{I}\\ \dfrac{J\cdot EI}{4\rho+J}K_{ww}^{-1}M_{ww} & 0 & 0 & 0\end{bmatrix},\quad B=\begin{bmatrix}0\\ 0\\ 0\\ -\dfrac{\rho\cdot EI}{4\rho+J}K_{ww}^{-1}F_r\end{bmatrix} \tag{27}$$

and $(\,)' \equiv \mathrm{d}/\mathrm{d}x$. It should be noted that the elements of $y(x)$ include the physical parameters of transverse deflection, transverse angle, mechanical moment, and shear force. Therefore, they play a crucial role in applying the boundary condition.

The response of the flexible appendage at any location is obtained by solving equation (26) as follows:

$$y(x) = \mathrm{e}^{A(l-x)}y(r) + \int_r^x \mathrm{e}^{A(x-\zeta)}B\zeta\,\mathrm{d}\zeta. \tag{28}$$

The above equation shows that the time history of the flexible motion consists of two individual contributions: (1) spatially propagated mechanical properties originating from the root of the appendage, and (2) the effect of the hub control torque combined with the eigenstructure characteristics of the flexible structure system. The motion of the tip of the flexible appendage can be obtained from:

$$y(l) = \Omega y(r) + \boldsymbol{\mu} \tag{29}$$

where

$$\Omega = e^{A(l-r)} \equiv \begin{bmatrix} \Omega_{11} & \Omega_{12} \\ \Omega_{21} & \Omega_{22} \end{bmatrix},$$

$$\boldsymbol{\mu} = \phi \Sigma(l) \Phi^{-1} B \equiv \Psi B,$$

$$\Sigma = \text{diag}\{\dots \ \sigma_i(x) \dots\},$$

$$\sigma_i(x) = e^{\lambda_i(x-r)} \left\{ \frac{r}{\lambda_i} + \frac{1}{\lambda_i^2} \right\} - \left\{ \frac{x}{\lambda_i} + \frac{1}{\lambda_i^2} \right\} \tag{30}$$

and λ_i and Φ are the ith eigenvalue and the modal matrix of the matrix A, respectively, and the square matrices Ω'_{ij}s $(i, j = 1, 2)$ are submatrices of Ω. Applying the boundary conditions, the unsolved mechanical properties at both ends are obtained as

$$\begin{bmatrix} M(r) \\ V(r) \end{bmatrix} = -\Omega_{22}^{-1} \boldsymbol{\mu}_2, \tag{31}$$

$$\begin{bmatrix} \mathbf{w}(l) \\ \mathbf{w}'(l) \end{bmatrix} = -\Omega_{12} \Omega_{22}^{-1} \boldsymbol{\mu}_2 + \boldsymbol{\mu}_1, \tag{32}$$

where $\boldsymbol{\mu} = [\boldsymbol{\mu}_1 \boldsymbol{\mu}_2]^T$. Note from equations (31) and (32) that all the state vectors are represented as a function of F_r. The slew motion can be obtained from the first row of equation (23) using the transverse deflection at the tip of the appendage

$$\theta = -\frac{\rho}{(J + 4\rho)} M_{ww}^{-1} F_r - \frac{4\rho}{l(J + 4\rho)} \mathbf{w}(l). \tag{33}$$

Thus, all the spatial distribution of the mechanical characteristics on the slewing appendages can be determined by equation (28).

3.2. GALERKIN'S WEAK PRINCIPLE

In this section, Galerkin's weak principle is used to model the hub–appendage system. In this modelling method, the constructed matrix equation includes the integration of the transverse deflection vector, and therefore, a more complicated formulation for spatial propagation results.

3.2.1. *Time discretization*

The following equations of motion can be obtained for the coupled slew-flexible motion [8]:

$$\rho \ddot{w}(x, t) + \rho x \ddot{\theta} + \frac{\partial^2}{\partial x^2} \left\{ EI \frac{\partial^2 w(x, t)}{\partial x^2} \right\} = 0, \tag{34}$$

$$J_h \ddot{\theta}(t) + 4 \int_r^l \rho x [\ddot{w}(x, t) + x \ddot{\theta}(t)] \, dx = u_r(t). \tag{35}$$

Multiplying equation (34) by $v(x, t)$, integrating over finite time, and integrating by parts yields

$$\int_{t_0}^{t_f} \rho w(x, t) \dot{v}(x, t) \, dt - \int_{t_0}^{t_f} \rho x \dot{\theta}(t) \dot{v}(x, t) \, dt + \int_{t_0}^{t_f} EI w^{(iv)}(x, t) \dot{v}(x, t) \, dt = 0. \tag{36}$$

Using the same shape functions for both $w(x, t)$ and $v(x, t)$, we obtain the following matrix ordinary differential equation:

$$-M_{ww}\mathbf{w}(x) - M_{ww}\boldsymbol{\theta}x + K_{ww}\mathbf{w}^{(iv)}(x) = 0. \tag{37}$$

The matrix equation for the slew mode can be obtained by a similar approach. However, the equation is of the algebraic type because the slew mode does not have any independent variables on the spatial domain.

$$-\frac{J_{tot}}{\rho}M_{ww}\boldsymbol{\theta} - 4M_{ww}\int_r^l x\mathbf{w}(x)\,\mathrm{d}x = F_r, \tag{38}$$

where F_r is redefined as

$$[F_r]_i = \int_{\Delta t} u_r(t)\,\phi_i(t)\,\mathrm{d}t$$

and $J_{tot} = J_h + 4\rho\,(l^3 - r^3)/3$.

3.2.2. *Spatial propagation*

Using the time domain finite element method, the equations of motion of the hybrid co-ordinate systems can be represented as shown in equations (37) and (38). Equation (37) represents the spatial propagation of the flexible mode. It is quite similar to that of the flexible beam, which is a fourth order matrix ordinary differential equation of spatial variable. Note that the slewing variable $\boldsymbol{\theta}$ and the structural deformation vector $\mathbf{w}(x)$ are coupled through equations (37) and (38), from which information on the slewing motion can be extracted. The control torque included in equation (38) affects the flexible mode in integral form.

The same state space formulation, as shown in equation (26) can be obtained for the flexible mode with only a small change, i.e.,

$$A = \begin{bmatrix} 0 & \mathbf{I} & 0 & 0 \\ 0 & 0 & \dfrac{1}{EI}\mathbf{I} & 0 \\ 0 & 0 & 0 & \boldsymbol{I} \\ EIK_{ww}^{-1}M_{ww} & 0 & 0 & 0 \end{bmatrix}, \quad B = \begin{bmatrix} 0 \\ 0 \\ 0 \\ EIK_{ww}^{-1}M_{ww}\boldsymbol{\theta} \end{bmatrix}. \tag{39}$$

And, a similar spatial propagation formulation for the flexible mode can be obtained. Now, let us analyze the slew motion of the hybrid co-ordinate systems starting from equation (38). To obtain the solution, the integration $\int_r^l x\mathbf{w}(x)\,\mathrm{d}x$ should first be transformed into a function of $\boldsymbol{\theta}$. The following equation can be obtained using equations (28) and (29):

$$\begin{aligned} \int_r^l xy(x)\,\mathrm{d}x &= \int_r^l \mathrm{e}^{A(x-r)}xy(r)\,\mathrm{d}x + \int_r^l \Phi\Sigma(x)x\Phi^{-1}B(\boldsymbol{\theta})\,\mathrm{d}x \\ &= \Phi\Theta(l)\Phi^{-1}y(r) + \Phi\Xi\Phi^{-1}B(\boldsymbol{\theta}), \end{aligned} \tag{40}$$

where Θ and Ξ are diagonal matrices whose diagonal terms are represented as follows:

$$\Theta_{ii} = \mathrm{e}^{\lambda_i(l-r)}\left\{\frac{l}{\lambda_i} - \frac{1}{\lambda_i^2}\right\} - \left\{\frac{r}{\lambda_i} - \frac{1}{\lambda_i^2}\right\}, \tag{41}$$

$$\Xi_{ii} = -\left\{\frac{l^3 - r^3}{3\lambda_i} + \frac{l^2 - r^2}{2\lambda_i^2}\right\} + \left\{\frac{r}{\lambda_i} + \frac{1}{\lambda_i^2}\right\}\left\{\mathrm{e}^{\lambda_i(l-r)}\left(\frac{l}{\lambda_i} - \frac{1}{\lambda_i^2}\right) - \left(\frac{r}{\lambda_i} - \frac{1}{\lambda_i^2}\right)\right\}. \tag{42}$$

TABLE 1

Configuration parameters for the hybrid co-ordinate systems

Parameter	Value	Units
Radius of hub	0·2000	m
Rotary inertia of hub	1·2732	kg m^2
Mass density of appendage	2800	kg/m^3
Young's modulus of appendage	$7{\cdot}5842 \times 10^{10}$	N/m^2
Thickness of appendage	0·0020	m
Width of appendage	0·0635	m
Length of appendage	0·8100	m

Therefore, $\int_r^l x\mathbf{w}(x)\,\mathrm{d}x$ can be expressed using the boundary conditions

$$\int_r^l x\mathbf{w}(x)\,\mathrm{d}x = \{\Pi_{11,44} - \Gamma_{11,34}\Omega_{22}^{-1}\Psi_{34,44}\}K_{ww}^{-1}M_{ww}\boldsymbol{\theta}, \tag{43}$$

where

$$\Pi = \Phi\Xi\Phi^{-1}, \quad \Gamma = \Phi\Theta(l)\Phi^{-1} \tag{44}$$

and $\Pi_{ij,kl}$, $\Gamma_{ij,kl}$, $\Psi_{ij,kl}$ are submatrices consisting of ij-rows and kl-columns of the matrices Π, Γ and Ψ, respectively, when the individual matrix is divided into 4×4 square submatrices. Finally, the time response of the slewing mode can be determined from the following equation:

$$\boldsymbol{\theta} = -\left\{\frac{J_{tot}}{\rho}M_{ww} + 4M_{ww}(\Pi_{11,44} - \Gamma_{11,34}\Omega_{22}^{-1}\Psi_{34,44})\,K_{ww}^{-1}M_{ww}\right\}^{-1}F_r \tag{45}$$

and the motion of the appendage can be obtained from equations (28) and (45) with equation (31).

3.3. NUMERICAL EXAMPLE

Numerical analysis was performed to validate the proposed modelling methods. All the results were compared with those obtained by the conventional spatial domain finite element method using numerical integration. The configuration parameters of the hybrid co-ordinate systems are listed in Table 1. Figures 6–8 show the comparative results for the slew angle, tip deflection of the appendage, and time history of the overall appendage respectively. The maneuver shown in the figures is based on torque shaping using the Fourier series optimization method [27]

$$u_r(t) = \sum_{i=1}^{7} a_i \sin\frac{\mathrm{i}\pi t}{t_f/2}$$

with $t_f = 3{\cdot}22$ s, and the coefficients a_i of the series expansion listed in Table 2. Note that the rest-to-rest maneuver guarantees zero initial displacement in both slew and flexible modes. Second order Lagrange polynomials are used for the time basis functions and 83 time finite elements are used with the time interval $\Delta t = 0{\cdot}06$ s. Figure 6 shows the slew angle, which shows good results for both modelling methods. However, we can see some discrepancy in the flexible mode between the method based on extended Hamilton's principle and the exact solution, as shown in Figures 7 and 8. This small mismatch results from the expansion of the

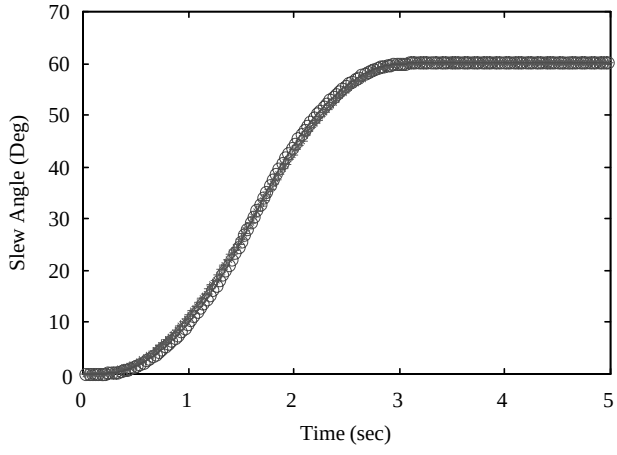

Figure 6. Slew angle history: * using Galerkin's weak principle; ** using extended Hamilton's principle: ○ time domain FEM*; * time domain FEM**; —— numerical simulation.

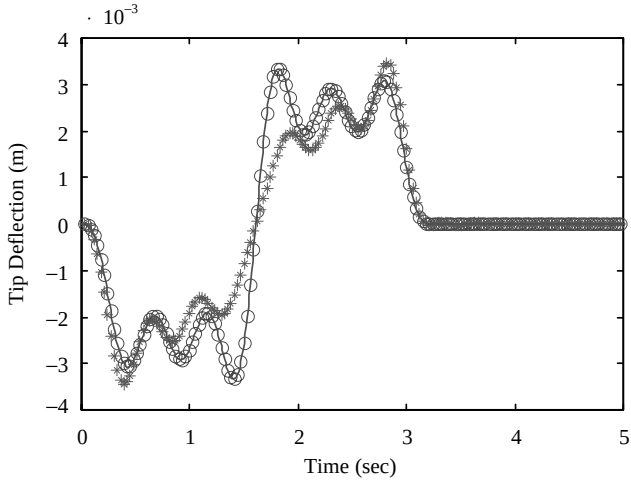

Figure 7. Tip displacement history: * using Galerkin's weak principle; ** using extended Hamilton's principle: ○ time domain FEM*; * time domain FEM**; —— numerical simulation.

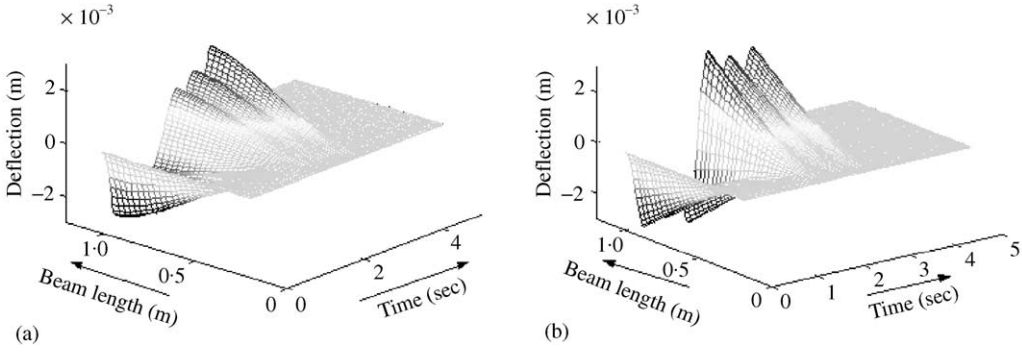

Figure 8. Spatial wave propagation: (a) using extended Hamilton's principle; (b) using Galerkin's weak principle.

TABLE 2

Optimized input shaping parameters

i	1	2	3	4	5	6	7
a_i	1·1180	− 0·0857	0·2714	− 0·1437	− 0·0731	− 0·1680	− 0·0006

equation to the spatial domain by applying the extended Hamilton's principle rather than the numerical error or the misled spatial propagation. That is, the obtained solution for the approximate slew motion [equation (18)] satisfies the variational relationship only in the overall sense. However, the error in the flexible motion is small enough to confirm the trend of the flexible motion. The error in slew motion is negligible within the boundary of the transverse deflection weighted by the mechanical properties of the hybrid co-ordinate systems. Using the relationship of equation (23), the upper half of equation (23) can be expressed as follows:

$$\boldsymbol{\theta} = -\frac{\rho}{4\rho + J} M_{ww}^{-1} F_r - \frac{4\rho}{4\rho + J} \frac{w(x)}{x}. \tag{46}$$

The second term of the above equation represents the influence of the flexible motion upon the slew history, while the first part is driven by the application of the external torque. At the root of the appendage, there is no flexural motion, which negates the effect of the second term. At the tip of the appendage, the flexible motion has a maximum effect upon the slew response with a value of $(4\rho/(4\rho + J))(w(l)/l)$. It reaches a maximum at the tip since the flexible appendage is governed by the lowest structural mode for the slew response excited by the shaped torque. However, the value is very small compared with the slew response caused by the external torque (the ratio of the second term to the first term is $9{\cdot}4 \times 10^{-4}$). Therefore, the effect of disturbing flexible motion in slew history is negligible and an accurate result can be obtained.

The modelling method could be used as an approximate solution when an appropriate control scheme has been developed. Moreover, it has a simple form and enables the computation of slew motion using the flexible mode, which gives a direct first estimate of the slewing and flexible motion. On the other hand, the modelling method based on Galerkin's weak principle can accurately describe the dynamic motion of a system, and can be applied to find accurate dynamic solutions using some complicated mathematical manipulations.

4. CONCLUSIONS

Several modelling methods were studied for the analysis of various dynamic systems using the time-domain finite element method. The general second order mechanical systems are modelled using Galerkin's weak principle and are verified by a simple pendulum example. The results are compared with those obtained using Hamilton's weak principle and it is shown that the proposed method exactly describes the dynamics of the open- and closed-loop systems with state feedback. The problem caused by the approximation of terminal momentum is also analyzed. Results from the dynamic systems analysis can be used for the dynamic modelling of more complicated mechanical systems.

Extending the results of non-propagating system modelling methods, various dynamic analysis methods are also proposed for hybrid co-ordinate systems that have both slew and flexible motions. The proposed methods are based on the extended Hamilton's principle

and Galerkin's weak principle, and the resulting equation of motion is spatially propagated to satisfy the boundary conditions at both ends, completing the dynamic analysis of the overall time and space solutions. A numerical example is shown to demonstrate the proposed methods. Modelling based on the extended Hamilton's principle shows some erroneous results for flexible motion, while the modelling based on Galerkin's weak principle shows the exact description of both slew and flexible modes. Therefore, it can be concluded that modelling based on Galerkin's weak principle is more likely to be used for the accurate analysis of hybrid co-ordinate systems.

Modelling based on the extended Hamilton's principle can also be used to produce a first estimate on what the slew and flexible motions would be expected to be when a new regulated control method is developed. In view of its relative simplicity in terms of the derivation of slew motion, the modelling method can be used as an approximate analysis tool for the slew and vibration analysis of hybrid co-ordinate systems. The modelling methods proposed in this paper can also be readily applied to trimmed rotational bodies where the initial momentum is identical to the final momentum of the system in a single period.

REFERENCES

1. C. Bailey 1975 *American Institute of Aeronautics and Astronautics Journal* **13**, 1154–1157. Application of Hamilton's law of varying action.
2. T. Simkins 1978 *American Institute of Aeronautics and Astronautics Journal* **16**, 559–563. Unconstrained variational statements for initial and boundary value problems.
3. M. Baruh and R. Riff 1982 *American Institute of Aeronautics and Astronautics Journal* **20**, 687–692. Hamilton's principle, Hamilton's law-6n correct formulations.
4. R. Riff and M. Baruh 1984 *American Institute of Aeronautics and Astronautics Journal* **22**, 1310–1318. Time finite element discretization of Hamilton's law of varying action.
5. R. Riff and M. Baruh 1984 *American Institute of Aeronautics and Astronautics Journal* **22**, 1171–1173. Stability of time finite elements.
6. M. Borri, G. Ghiringhelli, M. Lanz, P. Mantegazza, and T. Merlini 1985 *Computers and Structures* **20**, 495–508. Dynamic response of mechanical systems by a weak Hamiltonian formulation.
7. D. H. Hodges and R. R. Bless 1992 *Journal of Guidance, Control, and Dynamics* **14**, 148–156. Weak Hamiltonian finite element method for optimal control problems.
8. S. Lee and Y. Kim 1997 *Journal of Guidance, Control, and Dynamics* **20**, 97–103. Time domain finite element method for inverse problem of aircraft maneuvers.
9. M. S. Warner and D. H. Hodges 2000 *Journal of Guidance, Control, and Dynamics* **23**, 86–94. Solving optimal control problems using hp-version finite element in time.
10. S. J. Kim and J. Y. Cho 1997 *American Institute of Aeronautics and Astronautics Journal* **35**, 172–177. Penalized weighted residual method for the initial value problems.
11. H. Öz and E. Adigüzel 1995 *Journal of Sound and Vibration* **179**, 697–710. Hamilton's law of varying action, Part I: assumed time-mode method.
12. H. Öz and E. Adigüzel 1995 *Journal of Sound and Vibration* **179**, 711–724. Hamilton's law of varying action, Part II: Direct optimal control of linear systems.
13. H. Öz and J. K. Ramsey 2000 *Journal of Sound and Vibration* **231**, 1189–1219. Time modes and linear systems.
14. O. P. Agrawal and V. R. Sonti 1996 *Journal of Sound and Vibration* **192**, 399–412. Modelling of stochastic dynamic systems using Hamilton's law of varying action.
15. J. L. Junkins and H. Bang 1993 *Journal of Guidance, Control, and Dynamics* **16**, 668–676. Maneuver and vibration control of hybrid coordinate systems using Lyapunov stability theory.
16. J. L. Junkins and J. D. Turner 1986 *Optimal Spacecraft Rotational Maneuvers*. Amsterdam: Elsevier.
17. C. I. Bajer 1986 *International Journal for Numerical Methods in Engineering* **23**, 2031–2048. Triangular and tetrahedral space–time finite elements in vibration analysis.
18. L. J. Hou and D. A. Peters 1994 *Journal of Sound and Vibration* **173**, 611–632. Application of triangular space-time finite elements to problems of wave propagation.

19. R. P. S. HAN and J. LU 1999 *Journal of Sound and Vibration* **222**, 65–84. A space–time finite element method for elasto-plastic shock dynamics.
20. A. H. VON FLOTOW and B. SCHAFER 1986 *Journal of Guidance, Control, and Dynamics* **9**, 673–680. Wave-absorbing controllers for a flexible beam.
21. A. YOUSEFI-KOMA and G. VUKOVICH 1996 *American Institute of Aeronautics and Astronautics Paper* 96-3759. A global wave absorbing controller for smart structures.
22. H. FUJII, T. OHTSUKA and T. MURAYAMA 1992 *Journal of Guidance, Control, and Dynamics* **15**, 431–439. Wave-absorbing control for flexible structures with noncollocated sensors and actuators.
23. H. FUJII, K. NAKAJIMA and K. MATSUDA 1996 *Journal of Guidance, Control, and Dynamics* **19**, 578–583. Wave approach for control of orientation and vibration of a flexible structure.
24. J. SUK and Y. KIM 1998 *American Institute of Aeronautics and Astronautics Journal* **36**, 1312–1320. Time domain finite element analysis of dynamic systems.
25. E. B. BECKER, G. F. CAREY and J. T. ODEN 1981 *Finite Elements: An Introduction*, Vol. 1. Englewood Cliffs, NJ, Prentice-Hall.
26. J. L. JUNKINS and Y. KIM 1993 *Introduction to Dynamics and Control of Flexible Structures, AIAA Education Series.* Washington, DC: American Institute of Aeronautics and Astronautics.
27. J. SUK, J. MOON and Y. KIM 1998 *Journal of Guidance, Control, and Dynamics* **21**, 698–703. Torque shaping using trigonometric series expansion for slewing of flexible structures.